

Access of Extracellular Cations to their Binding Sites in Na,K-ATPase: Role of the Second Extracellular Loop of the α Subunit

Oihana Capendeguy,¹ Pierre Chodanowski,² Olivier Michielin,^{2,3,4} and Jean-Daniel Horisberger¹

¹Department of Pharmacology and Toxicology, University of Lausanne, Faculty of Biology and Medicine, CH-1005 Lausanne, Switzerland

²Swiss Institute of Bioinformatics, Bâtiment Ecole de Pharmacie, Université de Lausanne, CH-1015 Lausanne, Switzerland

³Ludwig Institute for Cancer Research /Lausanne Branch, CH-1066 Epalinges, Switzerland

⁴Centre Pluridisciplinaire d'Oncologie, Centre Hospitalier Universitaire Vaudois Lausanne, CH-1011 Lausanne, Switzerland

Na,K-ATPase, the main active transport system for monovalent cations in animal cells, is responsible for maintaining Na^+ and K^+ gradients across the plasma membrane. During its transport cycle it binds three cytoplasmic Na^+ ions and releases them on the extracellular side of the membrane, and then binds two extracellular K^+ ions and releases them into the cytoplasm. The fourth, fifth, and sixth transmembrane helices of the α subunit of Na,K-ATPase are known to be involved in Na^+ and K^+ binding sites, but the gating mechanisms that control the access of these ions to their binding sites are not yet fully understood. We have focused on the second extracellular loop linking transmembrane segments 3 and 4 and attempted to determine its role in gating. We replaced 13 residues of this loop in the rat $\alpha 1$ subunit, from E314 to G326, by cysteine, and then studied the function of these mutants using electrophysiological techniques. We analyzed the results using a structural model obtained by homology with SERCA, and ab initio calculations for the second extracellular loop. Four mutants were markedly modified by the sulfhydryl reagent MTSET, and we investigated them in detail. The substituted cysteines were more readily accessible to MTSET in the E1 conformation for the Y315C, W317C, and I322C mutants. Mutations or derivatization of the substituted cysteines in the second extracellular loop resulted in major increases in the apparent affinity for extracellular K^+ , and this was associated with a reduction in the maximum activity. The changes produced by the E314C mutation were reversed by MTSET treatment. In the W317C and I322C mutants, MTSET also induced a moderate shift of the E1/E2 equilibrium towards the E1 (Na) conformation under Na/Na exchange conditions. These findings indicate that the second extracellular loop must be functionally linked to the gating mechanism that controls the access of K^+ to its binding site.

INTRODUCTION

Na,K-ATPase is a membrane protein present in all animal cells. It is a member of the P-type ATPase family that uses the energy provided by ATP hydrolysis to drive three Na^+ ions out of the cell and drive two K^+ ions into the cell. Na,K-ATPase is responsible for maintaining the electrochemical gradient of Na^+ and K^+ ions across the plasma membrane, which is necessary for regulating cell volume, for maintaining the resting membrane potential in excitable cells, and for many secondary active transport systems. The functional enzyme is a heterodimer with a large catalytic α subunit (~ 110 kD) including 10 transmembrane segments (M1–M10) associated with a glycosylated β subunit (~ 55 kD) that crosses the membrane once (Horisberger, 2004). The α subunit contains the ATPase catalytic site, the binding sites for cations and for ouabain, a specific inhibitor of Na,K-ATPase. The structure of the sarcoplasmic reticulum Ca^{2+} -ATPase (SERCA) has been determined at high resolution (Toyoshima et al., 2000; Sorensen et al., 2004;

Toyoshima and Inesi, 2004), but no atomic resolution structure is yet available for Na,K-ATPase. Structural models of Na,K-ATPase have been obtained by homology with SERCA, and two cation binding sites for Na^+ and K^+ implicating M4, M5, and M6 have been proposed at locations homologous to the calcium-binding sites in SERCA (Ogawa and Toyoshima, 2002). The findings of a number of experimental mutagenesis studies support the same locations for Na^+ and K^+ binding sites (Jorgensen et al., 2003). A third binding site for Na^+ , initially proposed on the basis of homology modeling (Ogawa and Toyoshima, 2002), has also recently been shown to be involved in Na^+ binding and its release on the extracellular side of the membrane (Li et al., 2005). The mechanism behind the transportation of cations by Na,K-ATPase across the plasma membrane is based on a cyclic scheme involving two main conformations, E1 and E2, in which cation binding sites are accessible either from the intracellular side (in the E1

Correspondence to J.-D. Horisberger:
Jean-Daniel.Horisberger@unil.ch

Abbreviations used in this paper: DTT, dithiothreitol; MTSET, (2-[trimethylammonium] ethyl) methanethiosulfonate bromide; SERCA, sarcoplasmic reticulum Ca^{2+} -ATPase; WT, wild-type.

conformation) or from the extracellular side (in the E2 conformation) (Apell and Karlish, 2001). According to the “alternating-access” mechanism, two gates, one on the intracellular side and one on the extracellular side, control access to the binding sites. These gates are never both open at once, but the internal gate opens during the E1 conformation to allow access from the intracellular side, and the external gate is open in the E2 conformation to allow access from the extracellular side. After cation binding there is a state during which both gates are closed; this is known as the cation-occluded state, and during this state, occluded ions do not have access to either side of the membrane.

Although homology modeling to different conformations of the SERCA has helped to provide a better understanding of cation transportation by Na,K-ATPase, the access pathway to the cation binding site, and the “gating” mechanisms that control the access of cations to their binding sites have not been completely elucidated. In studies of the release of ^{86}Rb from Na,K-ATPase, Forbush (1987) proposed a “flickering gate” model, in which a rapidly opening and closing gate controls the access of individual extracellular K^+ ions to their binding sites. In a previous study in which we determined cysteine accessibility and the effects of mutations on extracellular K^+ affinity, we demonstrated the importance of the third extracellular loop (between M5 and M6) in allowing external K^+ ions access to their binding sites. Homology modeling indicates that this loop is very short and located rather deeply. This means that it is unlikely that this third loop can be the only structure responsible for the external gate. To improve our understanding of how access to K^+ binding sites is controlled from the extracellular side, we have now targeted the second extracellular loop that links M3 and M4. According to homology modeling, this loop covers part of the cation channel, and a physiologically significant displacement of the third and fourth transmembrane segments occurs during the E1.Na $^+$ →E2 conformation change. It has also been suggested that this loop may constitute the luminal gate in the SERCA calcium pump (Toyoshima and Nomura, 2002).

To investigate the role of the second extracellular loop in regulating the access of extracellular K^+ ions to their binding sites, we replaced the residues in this loop and in the first part of the fourth transmembrane segment (residues E314 to G326) by cysteine. Using electrophysiological techniques, we first studied the functional expression of these mutants by monitoring their response to external K^+ and ouabain. We then used a membrane-impermeant thiol reagent to assess the accessibility of these positions under different ionic conditions in order to detect structural differences between the E1 and E2 conformations. Finally, in order to investigate the role of this part of the protein in controlling the access of cations to their binding site, we have

characterized the effects of these mutations and of (2-[trimethylammonium] ethyl) methanethiosulfonate bromide (MTSET) binding on the apparent affinity for external K^+ , and on the kinetics of the binding and release of external Na^+ .

MATERIALS AND METHODS

Oocytes

Female *Xenopus laevis* toads were anesthetized with tricaine MS 222 (2 g.l $^{-1}$; Sandoz). Parts of the ovaries were removed through a 1-cm ventral incision. These procedures were approved by the Service Vétérinaire Cantonal of the Canton of Vaud. Fragments of ovaries were treated with collagenase. The oocytes were then incubated at 19°C in a modified Barth's solution containing (in mM) 85 NaCl, 2.4 NaHCO $_3$, 1 KCl, 0.8 MgSO $_4$, 0.3 CaNO $_3$, 0.4 CaCl $_2$, and 10 HEPES (pH 7.4), and supplemented with 10 mg/ml penicillin and 5 mg/ml streptomycin.

Site-directed Mutagenesis

Cysteine mutants (E314C to G326C) were generated using the $\alpha 1$ subunit of the rat Na,K-ATPase subcloned into the pSD5 vector. The mutants were generated using the QuickChange site-directed mutagenesis kit of Stratagene. All mutations were confirmed by sequencing. Mutant rat $\alpha 1$ subunits and wild-type (WT) rat $\beta 1$ subunit cRNA were synthesized by in vitro transcription as previously described (Jaisser et al., 1992).

Expression of Rat Na,K-ATPase in *Xenopus* Oocytes

14 ng α subunit and 1.4 ng β subunit cRNA were mixed and injected together in a total volume of 50 nl into stage V–VI *Xenopus laevis* oocytes prepared as described previously (Geering et al., 1989). The oocytes injected were incubated for 3–4 d in modified Barth's solution, and loaded with sodium by incubating for 2 h in a K^+ -free and Ca^{2+} -free medium containing 80 mM Na $^+$ and 0.5 mM EGTA. They were then incubated overnight in a K^+ -free amphibian Ringer solution containing 0.2 μM ouabain to inhibit the endogenous *Xenopus* Na,K-ATPase. This concentration of ouabain makes it possible to study selectively the activity of the exogenously expressed rat Na,K pump, which is moderately ouabain resistant (Horisberger and Kharoubi-Hess, 2002).

Electrophysiological Measurements

Na $^+$ -loaded oocytes were studied using the two-electrode voltage-clamp technique. Voltage and current were recorded by a TEV-200 voltage clamp (Dagan) and analyzed with the pCLAMP data acquisition package (Axon Instrument). All experiments were performed at room temperature (22–25°C).

In each oocyte the Na,K pump current was activated by adding 10 mM K^+ to a previously K^+ -free solution (see composition of the control solution below), and the ouabain sensitive current was measured by adding 2 mM ouabain to the 10 mM K^+ solution. A holding membrane potential of -50 mV was maintained except for a series of 150-ms voltage steps from -130 up to $+30$ mV in 20-mV increments. Current/voltage (I/V) curves were established from the steady-state membrane currents recorded at the end of each voltage step (at ~ 130 ms). The Na,K pump current was calculated as the difference between the steady-state currents in the presence and in the absence of extracellular K^+ , and the current inhibited by ouabain was calculated as the difference between the steady-state currents recorded in the presence of extracellular K^+ before and after inhibition by 2 mM ouabain.

The composition of the Na $^+$ -containing control solution was (in mM) Na $^+$ 92.4, Mg $^{2+}$ 0.82, Ba $^{2+}$ 5, Ca $^{2+}$ 0.41, TEA $^+$ 10, Cl $^-$ 22.4, HCO $_3^-$ 2.4, HEPES 10, gluconate 80, pH 7.4; K^+ channel

blockers (Ba²⁺, TEA⁺) were used to minimize the effect of K⁺ on the K⁺ channel currents. For the Na⁺-free solution, the Na⁺ gluconate was replaced by NMDG chloride, resulting in the following solution (in mM): Na⁺ 92.4, Mg²⁺ 0.82, Ba²⁺ 5, Ca²⁺ 0.41, TEA⁺ 10, Cl⁻ 102.4, HEPES 10, pH 7.4.

Cysteine Accessibility

For each of the cysteine mutants, the Na,K pump current activated by 10 mM external K⁺ was measured before and after exposure for 2 min to a concentration of 250 μM MTSET. MTSET was added either in a 10 mM K⁺ solution with 100 mM external Na⁺ to promote the E1 conformation of the Na,K-ATPase or in a solution devoid of external K⁺ and Na⁺, to promote the E2 conformation, as discussed previously (Capendeguy and Horisberger, 2005).

Kinetics of the Activation of the Na,K pump by Extracellular K⁺

The activation of the Na,K pump current by external K⁺ was studied in two separate sets of experiments, in the presence and in the absence of external Na⁺ (Jaisser et al., 1994). In brief, K⁺-induced currents in presence of 100 mM external Na⁺ were recorded after a stepwise increase of the K⁺ concentration from 0.0 to 0.3, 1.0, 3.0, and 10 mM. In the absence of external Na⁺, the K⁺ concentrations were 0.0, 0.05, 0.1, 0.2, and 5 mM. I-V curves were recorded after stabilizing the current at each of the K⁺ concentrations. The current induced by K⁺ at each potential was obtained by subtracting the current measured in the K⁺-free solution from that measured in the presence of K⁺. The maximum K⁺-activated current (V_{max}), and the half-activation constant (K_{1/2} K⁺) were determined by fitting the Hill equation parameters to the K⁺ concentration-current curve using a Hill coefficient of 1.6 for measurements in the presence of Na⁺ and of 1.0 in the absence of Na⁺ (Jaisser et al., 1994).

Presteady-state Ouabain-sensitive Currents

To study the kinetics of Na⁺ transport and the E1/E2 conformational equilibrium, transient, ouabain-sensitive, presteady-state currents were recorded under Na⁺/Na⁺ exchange conditions, i.e., in a 100 mM Na⁺, K⁺-free solution as described earlier (Li et al., 2005). Fast voltage clamping was achieved using large diameter current-passing electrodes with a resistance of <1 MΩ. Current was recorded during a series of 50-ms voltage steps from -170 to +30 mV. To minimize noise, series of 10 runs were averaged. Two series of voltage steps were recorded at intervals of about 1 min before exposure to 2 mM ouabain and another two after this exposure. The data were used only if there was no significant difference between the pairs of measurements obtained with and without ouabain. The relaxation phase of the ouabain-sensitive current transients induced by voltage steps (starting 2–5 ms after the beginning of the voltage step) were fitted to a single exponential using the PClamp routine in order to determine its exponential rate constant (k), and to estimate the size of the ouabain-sensitive current at the start of the voltage step, I_{ou}(0), by extrapolation. The ouabain-sensitive charge displacement (Q) was then calculated as Q = I_{ou}(0)/k.

Reagents and Solutions

Ouabain (Fluka) was added (from a 2 mM stock solution in DMSO) at a concentration of 0.2 μM in K⁺-free amphibian Ringer solution. For the 2 mM concentration experimental solutions, ouabain was directly dissolved in the final solution. MTSET (Toronto Research Chemicals Inc.) was freshly prepared immediately before each experiment. MTSET was dissolved in H₂O at a concentration of 250 mM, and was kept on ice until it was added to the experimental solution to be perfused within the next few minutes. Dithiothreitol (DTT, threo-1,4-dimercapto-2,3-

butanediol) (Sigma-Aldrich) was added to a 1 M stock solution kept on ice.

Molecular Modeling

Homology models of Na,K-ATPase were constructed on the basis of the crystal structures of SERCA in the E1 state (Protein Data Bank code 1SU4) and E2 state (PDB code 1WPG), using the alignment and the protocol described previously (Horisberger et al., 2004).

M3–M4 Loop Modeling. According to the sequence alignment, the end of the M3 helix of Na,K-ATPase was considered to be L311, which corresponds to I276 for SERCA. The beginning of M4 helix was set to the W317 position in Na,K-ATPase, as in the case of SERCA (W288). The ILHYT sequence, between L311 and W317, was defined to be the M3M4 loop.

Conformational Space Search. Conformational sampling of the M3M4 loop was performed using a simulated annealing protocol described elsewhere (Fagerberg et al., 2006). In brief, 1,000 heating-cooling cycles followed by energy minimization were performed in a vacuum using a distance-dependent dielectric constant (ε = 4.r) to allow partially for the effect of the solvent.

Effective Energy Calculation. Each conformer was post-processed using a more elaborated force field taking into account accurately the contribution of the solvation free energy based on the Generalized Born using Molecular Volume approach. The effective energy was computed as by Fagerberg et al. (2006). The CHARMM program (Brooks et al., 1983) was used to perform the conformational sampling and the effective energy calculation.

Best Loop Candidate Selection. The conformers were clustered according to their RMSD values using graph theory clustering (Fagerberg et al., 2006). For each cluster, the Boltzmann weighted average of the effective energy of the cluster members was calculated, and the clusters ranked accordingly. The conformer with the smallest effective energy in the cluster of minimum Boltzmann average energy was selected as the best loop candidate. We provide in Table I the PROCHECK (Laskowski et al., 1993) Ramachandran plot quality results for the nine residues defining the anchor points and the loop in the E1 and E2 conformation of the NaK-ATPase rat model. For both conformations, the stereochemistry of the backbone for the nine residues is either in the most favored regions (A, B) or in the additional allowed regions (a, b).

Data Presentation and Statistics

Because the expression of exogenous Na,K-ATPase in oocytes is variable, current amplitude values are usually reported after normalizing in terms of the outward current induced by 10 mM K⁺ measured at -50 mV at the beginning of the experiment. We have shown previously that this yields an accurate estimate of the number of active Na,K pumps on the surface of the oocyte (Jaunin et al., 1992). Results are reported as mean ± SEM (n = number of measurements). Student's *t* test for unpaired data was used for the statistical comparisons between WT and mutant groups, and the Student's *t* test for paired data

TABLE I

Ramachandran Plot Quality Results Analysis (PROCHECK)

	S310	L311	I312	L313	E314	Y315	T316	W317	L318
E1 (1SU4)	A	A	B	B	A	B	B	A	A
E2 (1WPG)	b	A	B	B	a	b	b	A	A

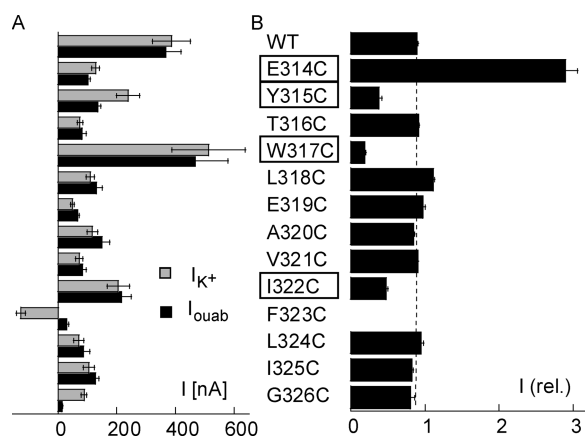


Figure 1. (A) Functional expression of Na,K-ATPase cysteine mutants. The K^+ -induced current (I_{K^+} , gray bars) and ouabain-sensitive current (I_{ouab} , black bars) are shown for oocytes injected with the cRNA of the $\beta 1$ and $\alpha 1$ subunits of the WT and cysteine mutants of residue positions 314–326 of the $\alpha 1$ subunit. Currents were recorded at -50 mV. Positive current values indicate an outward current. There were between 4 and 15 measurements in each group. (B) Effect of MTSET. The current measured after exposure to $250 \mu\text{M}$ MTSET for 2 min is reported after normalizing for the current measured before exposure to MTSET. There were between five and eight measurements in each case. The four mutants showing major modifications after MTSET treatment, and which were studied in greater detail, are highlighted.

was used for comparisons of the different responses obtained from the same oocyte (before and after cysteine reagent treatment, for instance).

RESULTS

Functional Expression of Cysteine Mutants and Effect of MTSET

The functional expression of each mutant (E314C to G326C) was studied by measuring the current induced by 10 mM K^+ and the current sensitive to 2 mM of ouabain in the presence of 10 mM of K^+ (Fig. 1 A). Except for the F323C mutant, all mutants showed a significant outward K^+ -induced current at -50 mV, ranging from 48 ± 6 nA, $n = 7$, for E319C to 513 ± 125 nA, $n = 11$, for the W317C mutant. The ouabain-sensitive current was similar to the K^+ -induced current for all the mutants except for the Y315C, F323C, and G326C mutants. As reported previously for the homologous mutant of the *Bufo marinus* Na,K-ATPase α subunit (Horisberger et al., 2004), K^+ induced an inward current for the F323C mutant, whereas the smaller ouabain-sensitive current in the Y315C and G326C mutants was most probably attributable to ouabain resistance. This hypothesis is supported by published evidence that these two residues are involved in ouabain binding; mutations of Y317 in the *Xenopus laevis* Na,K-ATPase α subunit (Y315 in our numbering) that reduced its sensitivity to ouabain (Canessa et al., 1993) and G319 (G326 in our numbering) was shown to

be one of the seven essential residues required to confer ouabain sensitivity on H,K-ATPase (Qiu et al., 2005).

As illustrated in the example in Fig. 3 A, the effect of MTSET was first studied by measuring the K^+ -activated current before and after exposure to $250 \mu\text{M}$ MTSET. As shown in Fig. 1 B, only 4 of the 12 mutants displayed a marked difference in their functional activity after MTSET exposure; E314C was markedly activated, whereas Y315C, W317C, and I322C were significantly inhibited by exposure to MTSET. For the other mutants, MTSET had little or no effect. Small effects could not be distinguished from the small decrease observed in WT, a decrease that could be attributed to a slow rundown of Na,K pump activity. Because our functional assays were not able to determine whether the absence of any effect of MTSET was due to the inaccessibility of the positions or to the absence of a functional consequence of binding to MTSET, the mutants displaying little or no effect of MTSET were not studied any further.

Accessibility of Cysteine to MTSET in the E1/E2 Conformations of Na,K-ATPase

The four mutants in which MTSET had a major functional effect were then studied further by recording the effects of the mutation itself and of MTSET binding on the kinetics of activation by extracellular K^+ .

To obtain a high level of inhibition, MTSET was first perfused for 2 min at a concentration of $250 \mu\text{M}$, and tested under conditions promoting the E1 or the E2 conformation of Na,K-ATPase by using an extracellular solution containing 100 mM Na^+ and 10 mM K^+ (promoting E1) or a Na^+ - and K^+ -free (promoting E2) extracellular solution. Fig. 2 A shows the amplitude of the K^+ -activated current after MTSET exposure normalized relative to its amplitude measured immediately before, for the WT and the four mutant Na,K-ATPases. For the E314C mutant, MTSET exposure resulted in a threefold increase of the K^+ -activated current, an increase that was not dependent on the conditions of MTSET exposure. In contrast, in the Y315C, W317C, and I322C mutants, MTSET exposure resulted in a significant decrease in the Na,K pump current in both conformations. Moreover, a statistically significantly greater inhibition was observed in the E1 conformation for these three mutants. The K^+ -induced current was inhibited by $63 \pm 5\%$, $n = 9$, under conditions promoting E1, vs. $51 \pm 4\%$, $n = 10$, for E2 ($P < 0.05$), for Y315C; by $84 \pm 1\%$, $n = 10$, in E1 vs. $76 \pm 1\%$, $n = 10$ ($P < 0.01$) for the W317C mutants; and by $56 \pm 3\%$, $n = 10$, in E1 vs. $25 \pm 1\%$, $n = 10$, in E2 ($P < 0.01$), for I322C.

To investigate more precisely the accessibility of the four positions, we performed similar measurements using a lower concentration of MTSET and a shorter exposure time. The MTSET concentration and exposure time were chosen on the basis of preliminary measurements in order to obtain approximately half of the

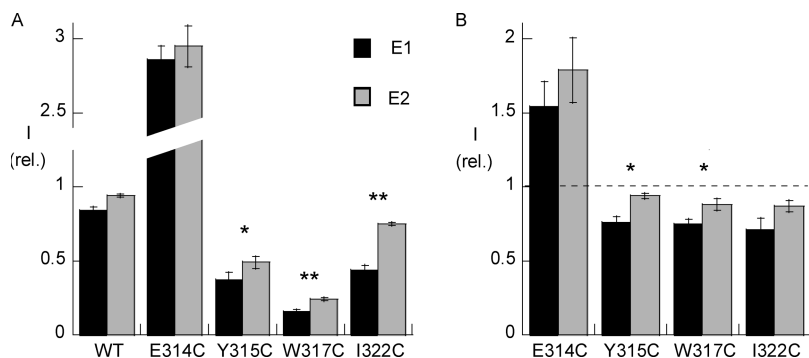


Figure 2. (A) Effects of MTSET on four Na,K-ATPase cysteine mutants: conformation-dependent effects. Means \pm SEM of K^+ -induced currents at -50 mV in oocytes expressing the cysteine mutants or WT α subunit. The currents, induced by adding 10 mM external K^+ to a 100 mM external Na^+ solution, measured after MTSET exposure are expressed after normalizing for the current measured before exposure to MTSET. MTSET was perfused for 2 min at a concentration of 250 μ M, either with 10 mM external K^+ , to shift the equilibrium toward the E1 conformation (black bars), or in a Na^+ -free and K^+ -free solution (gray bars), to promote the E2P conformation of the Na,K-ATPase. Between 9 and 10 measurements were performed for each condition. Error bars represent the SEM. The effect of MTSET was statistically significant ($P < 0.01$) for each mutant in the E1 conformation condition versus WT. *, $P < 0.05$; **, $P < 0.01$, for the comparison between the E1 and E2 conformation for the same mutant. (B) Effects of MTSET at low concentrations. For each mutant, the effect of a concentration that resulted in approximately half of the maximum effect was tested in the presence of Na^+ and K^+ . *, $P < 0.05$ for the comparison between the E1 and E2 conformation for the same mutant.

maximum effect in the presence of Na^+ and K^+ . Under these conditions, the level of inhibition observed after a short exposure time depends on the rate of inhibition. These measurements, shown in Fig. 2 B, indicate that for the Y315C and W317C mutants, the rate of inhibition was significantly greater in the E1 than in the E2 conformation.

Specificity of the MTSET Binding Effect

We also tested the reversibility of the effect of MTSET after exposure to DTT, a strong reducing agent. DTT was applied at a concentration of 10–50 mM for 2 min, and the Na,K pump current activated by 10 mM K^+ was measured again (see the example in Fig. 3 A). I/V curves were recorded before and after exposure to MTSET, and after applying DTT. Fig. 3 B summarizes the inhibitory (or stimulatory for E314C) effects of MTSET, and the recovery observed after exposure to DTT. In the W317C mutants, the K^+ -activated current had nearly completely recovered from MTSET inhibition, whereas recovery was only partial for the E314, I322C, and Y315C mutants.

Effects of MTSET on Activation by External K^+

As shown in Fig. 3 A for W317C, the effect of 250 μ M MTSET rapidly reached its maximal level, suggesting that even after full derivatization of the accessible cysteine, a residual function was still present. This was similar to what we have already reported for several mutants of the third extracellular loop (Capendeguy and Horisberger, 2005). This was also true of E314C and Y315C, whereas the effect on I322C was slower. We then studied the transport characteristics of Na,K-ATPase mutants E314C, Y315C, W317C, and I322C before and after a stationary effect of MTSET. We determined the apparent affinity for external K ($K_{1/2}K^+$) and the maximum activity (I_{max}) of the mutants before and after exposure to 250 μ M MTSET for 2 min.

Figs. 4 and 5 show the I_{max} and the $K_{1/2}K^+$ values as a function of the membrane potential when measured in the presence or absence of extracellular Na^+ ,

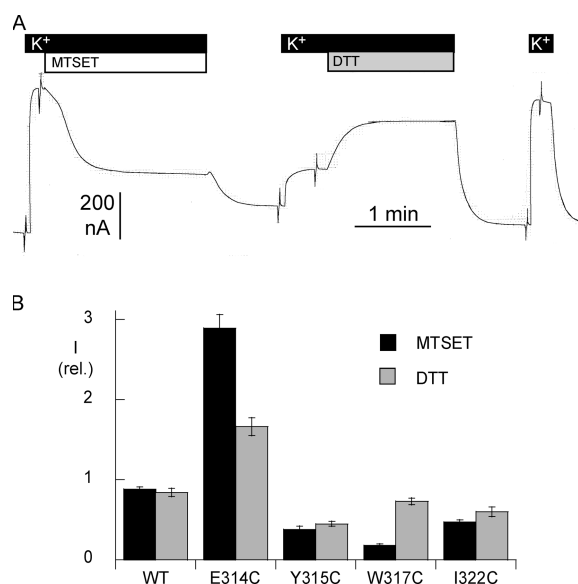


Figure 3. (A) Original current recordings in an oocyte expressing the W317C mutant of the $\alpha 1$ subunit of rat Na,K-ATPase. The holding membrane potential was kept at -50 mV, except for series of short voltage steps. The effect of MTSET was tested by measuring the K^+ -induced outward current before and after exposure to 250 μ M MTSET for 2 min. The reversibility of the effect of MTSET was tested by measuring the K^+ -induced outward current before and after exposure to 10 mM DTT for 2 min. (B) Reversibility of the effect of MTSET. The effect of a reducing agent, dithiotreitol (DTT), was measured as described in the examples above. The bar graphs report that amplitude of the K^+ -activated current after MTSET exposure (2 min, 250 μ M) and after subsequent DTT treatment (2 min, 10 mM). The current values are normalized in terms of the current measured under the initial control conditions. The DTT-induced recovery was complete the W317C mutant, but only partial in the E314C, Y315C, and I233C mutants. There were between five and seven measurements for each condition. Error bars represent the SEM.

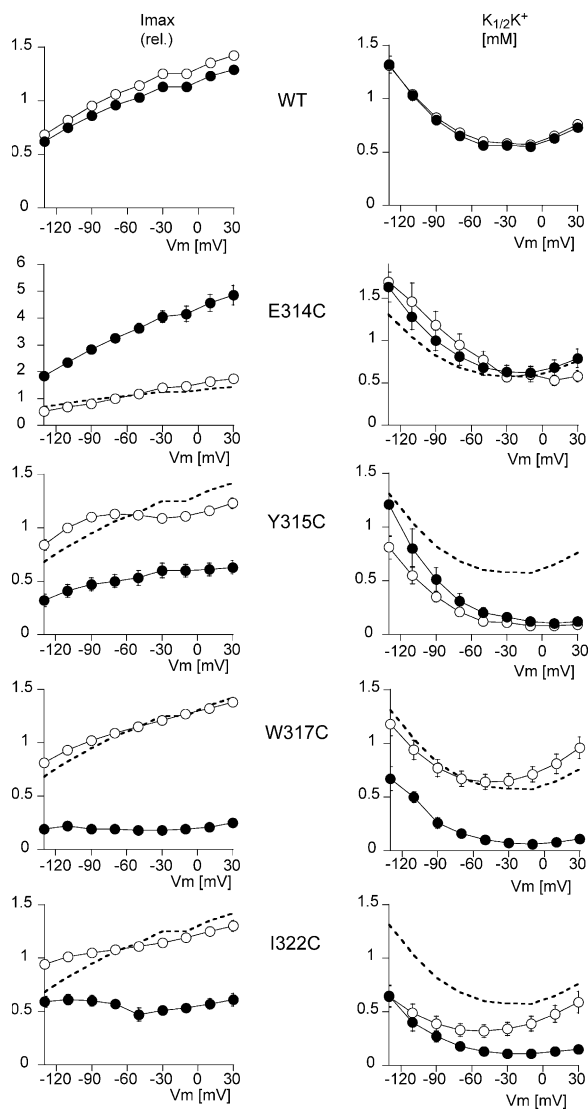


Figure 4. Effect of MTSET on the voltage-dependent kinetics of activation by extracellular K^+ . The K^+ concentration was increased in steps from 0 to 0.3, 1.0, 3.0, and 10 mM. MTSET was added at a concentration of 250 μ M to the 10 mM K^+ solution, and after a 2-min exposure, the K^+ -induced current was measured again by exposure to the same external K^+ concentrations. I-V curves were recorded for each K^+ concentration. The values of the K^+ -induced current at each concentration were used to calculate the maximum K^+ -induced current (I_{max}) and the K^+ activation constant ($K_{1/2}K^+$), as described in MATERIALS AND METHODS. The $K_{1/2}K^+$ values were obtained by recording I-V curves in increasing K^+ concentrations before and after exposure to MTSET. The five plots on the left represent the I_{max} and the five plots on the right the $K_{1/2}K^+$, as a function of the membrane potential for the WT ($n = 10$) and for four cysteine mutants, E314C ($n = 10$), Y315C ($n = 9$), W317C ($n = 10$), and I322C ($n = 10$). The curves with open symbols represent the measurements before MTSET perfusion, and those with the filled symbols represent the measurements after exposure to MTSET. The mean values measured in WT before MTSET treatment (open symbols in the top plot) are shown as a thick dashed line (without symbols or error bars) in the plots for each mutant for comparison. Error bars represent SEM. The error bars are smaller than the symbol size in some cases.

respectively. In the presence of extracellular Na^+ , WT Na,K-ATPase presented an I/V curve of the usual shape, with a slightly positive slope and a U-shaped voltage dependence for $K_{1/2}K^+$ (Jaisser et al., 1994). The $K_{1/2}K^+$ at -50 mV was 0.60 ± 0.02 mM ($n = 10$). Neither the apparent affinity nor the maximum activity of the WT was affected by exposure to MTSET. The small decrease by $\sim 15\%$, observed in I_{max} after exposure to MTSET, was always observed, and was due to a decrease in the functional activity over time. Apart from Y315C, the mutants also displayed a U-shaped voltage dependence curve with a $K_{1/2}K^+$ at -50 mV of 0.77 ± 0.1 mM ($n = 10$) for E314C, of 0.64 ± 0.07 mM ($n = 10$) for W317C, and of 0.32 ± 0.06 mM ($n = 10$) for I322C. In comparison to the WT enzyme, the I322C mutation increased the apparent external K^+ affinity about twofold, with a greater difference at negative than positive membrane potentials. Y315C was characterized by a marked increase in the apparent external K^+ affinity ($K_{1/2}K^+$ 0.12 ± 0.03 mM; $n = 9$ at -50 mV), and also displayed a monotonic voltage dependence, with $K_{1/2}K^+$ values that were higher at negative than at positive membrane potentials. After MTSET treatment, $K_{1/2}K^+$ was not significantly modified for E314C and Y315C, whereas it fell for the W317C mutant (from 0.64 ± 0.07 to 0.10 ± 0.02 mM; $n = 10$ at -50 mV, $P < 0.001$) and the I322C mutant (from 0.32 ± 0.06 to 0.13 ± 0.03 mM; $n = 10$ at -50 mV, $P < 0.001$). As shown above in Fig. 1, MTSET exposure increased the I_{max} of the E314C mutant by $186 \pm 9\%$, whereas it decreased the I_{max} of the Y315C, W317C, and I322C mutants by $63 \pm 5\%$, $84 \pm 1\%$, and $56 \pm 3\%$, respectively (values at -50 mV). The voltage dependence of the Na,K pump activity was not markedly modified.

In the absence of extracellular Na^+ (a condition under which the $K_{1/2}K^+$ more directly represents the intrinsic affinity of the K^+ binding site, without any interference from competing Na^+ binding, Fig. 5), we observed that the maximum current I/V relationship displayed a flat section at positive potentials, a negative slope at high negative membrane potentials, and monotonic voltage dependence of $K_{1/2}K^+$, as had previously been reported under similar conditions (Rakowski et al., 1991; Jaisser et al., 1994). The various mutations had effects on I_{max} that were qualitatively similar to those recorded in the presence of extracellular Na^+ , namely the stimulation of I_{max} in the case of E314C, and its inhibition for the other three mutations.

Similarly to what had been observed in the presence of Na^+ , there was no significant difference in $K_{1/2}K^+$ between W317C and WT before MSTET treatment, indicating that the apparent affinity for K^+ was not modified by the W317C mutation itself. In contrast, $K_{1/2}K^+$ values were reduced over the whole potential range by the E314C, Y315C, and I322C mutations, without any obvious modification of the voltage dependence of this

variable (shape of the $K_{1/2}K^+$ vs. V_m curve), indicating that these mutants had a higher apparent affinity for extracellular K^+ . The apparent affinity at -50 mV was the same for the W317C mutant ($K_{1/2}K^+$ 0.09 ± 0.01 mM, $n = 10$) as for WT ($K_{1/2}K^+$ 0.09 ± 0.01 mM, $n = 10$), but was increased for the E314C (0.029 ± 0.002 , $n = 12$), Y315C (0.025 ± 0.005 mM, $n = 9$), and I322C (0.044 ± 0.008 mM, $n = 11$) mutants.

MTSET treatment had no significant effect on WT ($K_{1/2}K^+$ 0.08 ± 0.01 mM, $n = 10$ at -50 mV) or Y315C (0.02 ± 0.005 mM, $n = 8$ at -50 mV), whereas it produced an increase in E314C (0.07 ± 0.01 mM, $n = 12$, $P < 0.01$, at -50 mV), restoring $K_{1/2}K^+$ to a value close to that of the WT. MTSET significantly reduced $K_{1/2}K^+$ for the W317C (to 0.03 ± 0.01 mM; $n = 10$ at -50 mV, $P < 0.01$) and I322C mutants (0.02 ± 0.01 mM; $n = 11$ at -50 mV, $P < 0.01$).

Effects of Mutations and MTSET Binding on the Kinetics of Na^+ Transport

The kinetics of the release/binding of extracellular Na^+ was studied by measuring the ouabain-sensitive, pre-steady-state currents following fast voltage perturbations under Na^+/Na^+ exchange conditions (Nakao and Gadsby, 1986; Rakowski, 1993). We studied the slow component of ouabain-sensitive, pre-steady-state current during 50-ms voltage steps (from -170 to $+30$ mV) in the WT and E314C, W317C, and I322C mutants. No measurements could be made for the Y315C mutant, because of its resistance to ouabain. The mean ouabain-sensitive charge displacement (Q), calculated as the time integral of the current transient, is shown in the panels on the left of Fig. 6. For each condition, the white and black curves represent the ouabain-sensitive charge displacement measured before and after MTSET treatment, respectively. The Q/V relation of the WT Na,K pump could be fitted to a Boltzmann relation with a Q_{max} of 2412 pC and a midpoint potential at -44 mV, which is compatible with published values (Li et al., 2005). MTSET had no effect on the WT charge displacement. The E314C mutant showed a reduced Q_{max} of 1056 pC, and a midpoint potential slightly shifted to the right at -32 mV. After MTSET binding, Q_{max} was increased to 3172 pC without any change in the midpoint potential. MTSET binding to the cysteine in position 314 restored the charge displacement quantity to close to the WT value. Finally, the W317C and I322C mutants showed a decrease in their Q_{max} after exposure to MTSET. After exposure to MTSET, the Q_{max} of W317C fell from 2523 pC to 1856 pC, and that of I322C from 1888 pC to 1426 pC. These changes were in the same direction, but quantitatively smaller than the reduction of the I_{max} reported above (see Fig. 2 A or Fig. 4). The decrease in Q_{max} was accompanied by a shift of the voltage dependence curve toward positive potentials ($V_{1/2}$ changed from -57 to

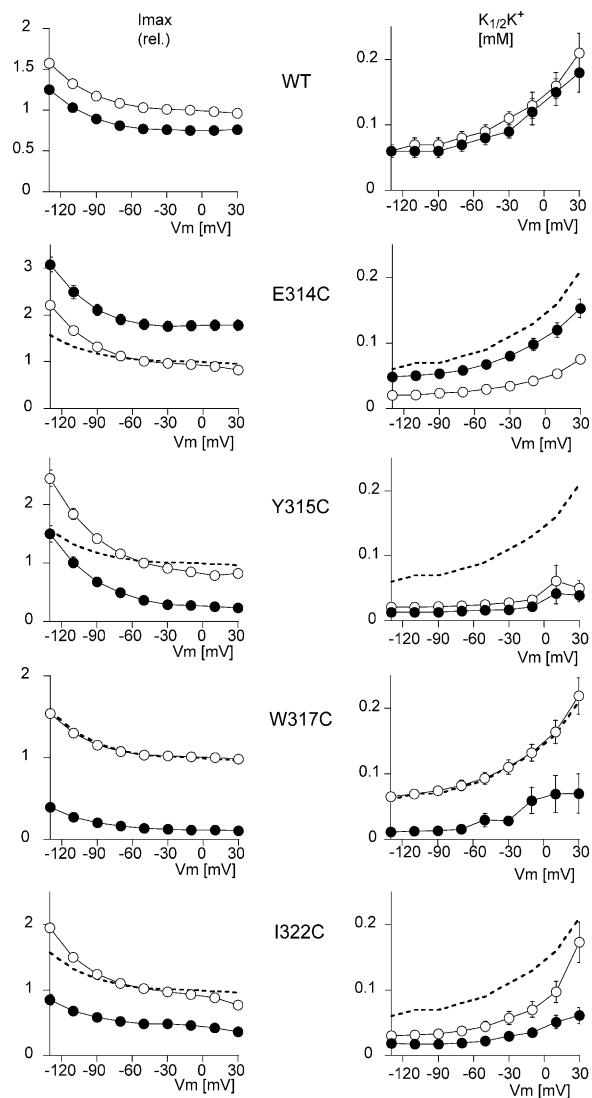


Figure 5. Effect of MTSET on the voltage-dependent kinetics of activation by extracellular K^+ in a Na^+ -free solution. The K^+ concentration was increased in steps from 0 to 0.05, 0.1, 0.2, and 5 mM. MTSET was added at a concentration of 250 μ M to the 5 mM K^+ solution, and after a 2-min exposure, the K^+ -induced current was measured again by exposure to the same external K^+ concentrations. I-V curves were recorded for each K^+ concentration. The values of the K^+ -induced current at each concentration were used to calculate the maximum K^+ -induced current (I_{max}), and the K^+ activation constant ($K_{1/2}K^+$), as described in MATERIALS AND METHODS. The $K_{1/2}K^+$ values were obtained by recording I-V curves in increasing K^+ concentrations before and after exposure to MTSET. The five plots on the left represent the I_{max} and the five plots on the right represent the $K_{1/2}K^+$ as a function of the membrane potential for the WT ($n = 10$) and for four cysteine mutants, E314C ($n = 12$), Y315C ($n = 9$), W317C ($n = 10$), and I322C ($n = 11$). The curves with open symbols represent the measurements before MTSET perfusion, and those with the filled symbols represent the measurements after exposure to MTSET. The mean values measured in WT before MTSET treatment (open symbols in the top plot) are shown as a thick dashed line (without symbols or error bars) in the plots for each mutant for comparison. Error bars represent SEM. The error bars are smaller than the symbol size in some cases.

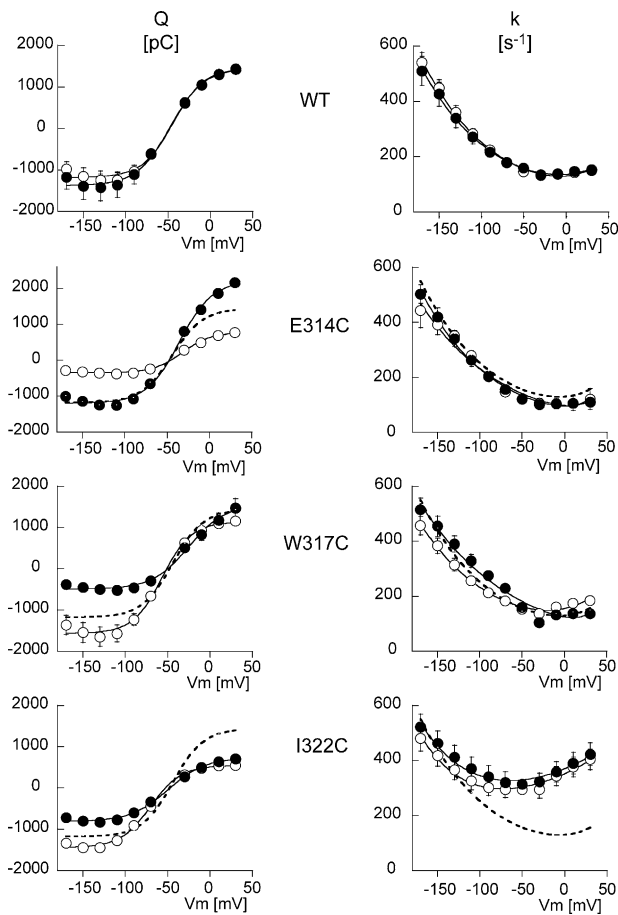


Figure 6. The slow component of the ouabain-sensitive, presteady-state currents under Na^+/Na^+ exchange conditions was measured before and after exposure to MTSET in WT and mutant Na,K-ATPases. The panels on the left show the voltage dependence of the ouabain-sensitive presteady-state charge translocation (Q). The smooth curves correspond to the best fitting Boltzmann equation:

$$Q(V) = Q_{\min} + Q_{\max} \left(1 + \exp\left(z(V_m - V_{1/2}) \frac{F}{RT}\right) \right)^{-1},$$

where $Q(V)$ is the charge displacement produced by the voltage step, Q_{\min} the charge displaced at the maximum negative membrane potential, Q_{\max} the maximum displaceable charge during a negative to positive potential jump, V_m the membrane potential, $V_{1/2}$ the midpoint potential, z the apparent valence, which was set to 1. F , R , and T have their usual meanings. The panels on the right show the voltage dependence of the relaxation rate of the slow component of the ouabain-sensitive presteady-state currents. The smooth curves show the best fitting curves corresponding to the following equation:

$$k(V) = k(0) \exp\left(-z \frac{VF}{RT}\right) + k'(0) \exp\left(z \frac{VF}{RT}\right),$$

which describes the voltage (V) dependence of the relaxation rate constant k as the sum of the forward and a backward voltage-sensitive rate constants with an effective charge z and values of $k(0)$ and $k'(0)$ at 0 mV, respectively. F , R , and T have their usual meanings. The curves with open symbols represent the measurements before MTSET perfusion, and those with the filled symbols represent the measurements after exposure to MTSET. The number of measurements was between four and eight. The mean values of Q and k , measured in WT before MTSET treatment (open symbols in the top plot), are shown as a thick dashed line (without symbols or error bars) in the plots for each mutant for comparison.

–25 mV and from –70 to –49 mV for the W317C and I322C mutants, respectively).

The voltage dependence of the relaxation rate (k) of the presteady-state current, shown in the panels on the right of Fig. 6, was similar to what has been reported previously (Nakao and Gadsby, 1986; Rakowski, 1993) in the WT and in the E314C and W317C mutants, with increasing rates at negative potentials, and little voltage dependence in the depolarized potential range. In addition, MTSET treatment had no detectable effect apart from a slight shift to the left of the voltage dependence curve for the W317C mutant. The I322C mutant displayed a U-shaped k/V relationship, with a marked increase in the relaxation rate in the depolarized potential range, with a shift of the minimum value of k (to around –60 mV). MTSET had no significant effect on this mutant either.

Ab initio Loop Modeling

The M3M4 loop conformations for the E1 and the E2 states are shown in Fig. 7. The two states have different loop conformations. This was to be expected, as the two states have, first, an anchor point separation distance difference of 4.3 Å and, second, a different environment for this loop. Indeed, the major conformational rearrangements in the transmembrane part between the E1 and E2 state involve the reorientation of the M1M2 and M3M4 part relative to the other transmembrane helices.

DISCUSSION

In an attempt to elucidate the “gating” mechanism that controls access from the extracellular solution to the cation binding sites of Na,K-ATPase, we studied the functional properties of cysteine mutants of residues located in the extracellular part of the second hairpin formed by the third and fourth transmembrane segments of the α subunit, and the functional effects induced by modifying the introduced cysteine residues with the membrane-impermeant cationic thiol reagent MTSET. The kinetics of the effects of MTSET were similar to what we have described previously (Capendeguy and Horisberger, 2005) and were, at least in part, reversed by exposure to DTT, suggesting that these effects were indeed due to the formation of a disulfide bond between MTSET and the protein. MTSET had no effects on any of the measured variables in the WT Na,K-ATPase, and we therefore assume that the effects of MTSET exposure were due to derivatization of the introduced cysteine residues. We have no documented explanation for the limited DTT-induced reversibility of the MTSET effect in the case of the Y315C and I322C mutants; for the deeply located C322, we hypothesize that derivatization of this residue may promote a

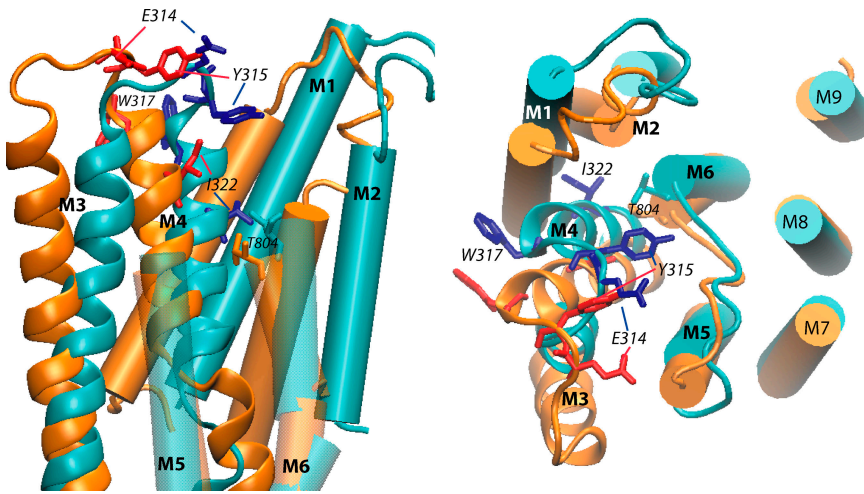


Figure 7. Structural model of the E1 and E2 states of the Na,K-ATPase built by homology with the 1SU4 and 1WPG structures of SERCA, respectively. The conformation of the loop was selected from among 500 conformers generated after clustering and effective energy calculation as detailed in MATERIALS AND METHODS section. The superposition was done on the fixed part of the TM domains between all the conformers. The distance between the helices in a given structure was calculated. We define one helix as being fixed relative to another if the distance considered is equal in all the structures (≤ 1.5 Å difference). Transmembrane segments (M1–M9) are indicated (in blue for E1 and in orange for E2). The M3–M4 hairpin is represented as thick ribbon representation with the side

chains of the four residues studied in details (E1 dark blue, E2 red). The panel on the left shows a view parallel to the membrane plane (extracellular side up) from the position of the transmembrane segments M7–M10, which have been removed for clarity. The M5–M6 loop is transparent and its extracellular part has been removed for clarity. The large outward movement of I322 from the E1 to the E2 conformation can be observed. The panel on the right shows a view from the extracellular side of the membrane; the large movements of E314, Y315, and W317 from the E1 to the E2 conformation can be observed. The large extracellular loop between M7 and M8 has been removed. The side chain of residue T804, at the top of segment M6, is shown.

conformation in which the residue becomes less accessible, but this explanation seems unlikely for C315 for which modeling indicates a water-accessible location. When MTSET exposure does not produce any functional modification, it cannot be determined from functional measurements alone, since whether the residue position is accessible to the reagent or the derivatization of a cysteine in this position or not has no functional consequences. We therefore restricted our analysis to four mutations on which MTSET exposure had a major impact, namely E314C, Y315C, W317C, and I322C. The positions of these residues are illustrated in Fig. 7.

In the following paragraphs we shall first consider the effects of each individual cysteine mutation and its MTSET derivatization before considering the global function of the second extracellular loop.

E314C

The case of the E314C mutation is remarkable in the sense that in contrast with all the other cases (>60 different cysteine mutants) that we have studied so far (Guennoun and Horisberger, 2000, 2002; Capendeguy and Horisberger, 2005), MTSET resulted in a large, roughly threefold increase in Na,K pump activity. It must first be noticed that the mutation itself resulted in a reduction in the maximum activity (I_{max}) (to $\sim 40\%$ of the WT value), a similar reduction of the total translocatable charge (Q_{max}), and an increase in the apparent affinity for extracellular K^+ measured in the absence of extracellular Na^+ (decrease of $K_{1/2}K^+$). We interpret these findings as indicating that the E314C mutant becomes partially trapped in an inactive conformation (resulting in the observed parallel decreases of I_{max}

and Q_{max}), and that it is freed when a charged group is added to this position.

Y315C

The accessibility of C315 fits in well with its position (similar to that of E314) close to the most extracellular position in the loop. This mutant has an extremely high apparent affinity for extracellular K^+ , which is most obvious in the absence of extracellular Na^+ (Fig. 5), when $K_{1/2}K^+$ directly represents the intrinsic affinity for extracellular K^+ , and MTSET binding does not affect this variable. The marked increase in $K_{1/2}K^+$ observed at high negative membrane potentials in the presence of extracellular Na^+ indicates that Na^+ competes with K^+ for binding to the same extracellular cation site, as observed for WT.

W317C

Even though W317 is conserved in all forms of Na,K-ATPase (and is replaced by another aromatic residue, phenylalanine, in gastric H,K-ATPase), cysteine substitution of this residue had little effect by itself on the Na,K pump function. Modeling indicates that W317 is located at the extracellular end of M4, with its side chain pointing toward the outside of the protein at the level of the membrane–extracellular solution interface, a position commonly occupied by aromatic residues (Killian and Von Heijne, 2000; Ulmschneider and Sansom, 2001; Granseth et al., 2005). MTSET induced a considerable (approximately fourfold) reduction in the maximal K^+ -activated current, together with a smaller reduction in Q_{max} , and a shift of the E1/E2 equilibrium toward E1 (detected as a 32-mV shift of the $V_{1/2}$ toward positive

potentials in the Na⁺/Na⁺ exchange mode, see Fig. 6). Aromatic and charged side chains of residues at the interface region have been shown to point in different directions, toward the membrane and away from the membrane, respectively (Chamberlain et al., 2004; Granseth et al., 2005). The change from an aromatic residue (W317) to a positively charged “pseudo residue” (MTSET-derivatized C317) can thus be expected to entail a marked structural change to the loop. It is interesting to compare these findings with those of Yudowski et al. (2003), who demonstrated a K⁺-sensitive effect of the isothiuronium derivative Br-TITU that they attributed to a strong interaction with an extracellular tryptophan residue. W317 (W310 in their numbering) was one of the proposed targets for this effect.

I322C

Among the four residues studied, I322C was the one for which the effect of MTSET was slowest, suggesting that it occupied a less readily accessible position. This residue is indeed located in the M4 helix rather than in the loop itself. In the E1 state it is located one helix turn below T804 (a threonine positioned at the top of the M6 helix) in the membrane, and its side chain points toward M1 and the membrane. However in the E2 state, it is located at the same level as T804 and the side chain points to M1 and the putative cation pathway. T804 has been shown to be readily accessible to both omeprazole and MTSET (Capendeguy and Horisberger, 2005), and seems to be located at the entrance of the narrowest, cation-selective part of the ion pathway (Artigas et al., 2005). The slower reactivity of C322 may be explained by the fact that its side chain is exposed to the solvent for only part of the time.

Modeling

Homology modeling of Na,K-ATPase on the basis of the SERCA structure has been very successful in determining the overall architecture of the α subunit, the detailed structure of the ATP binding site, the phosphorylation site, and at least some of the cation binding sites. The structure of the third extracellular loop was also easily modeled because of the high degree of sequence conservation in TM5 and TM6 and the absence of deletion/insertion differences between the SERCA and Na,K-ATPase sequences. Modeling the second extracellular loop has been more problematic because of a low degree of sequence homology, and above all because of a 10-residue difference in length between this loop in SERCA and in the Na,K-ATPase α subunit.

We have attempted to solve this problem by using *ab initio* modeling of the short, five-residue loop of Na,K-ATPase, while keeping the ends of this loop anchored in the much better conserved third and fourth transmembrane segment.

The efficiency of the sampling, scoring, and clustering methods used in this work has been assessed by Fagerberg et al. (2006). The conformational sampling of the second extracellular loop was performed using a computationally cheap force field while the conformer ranking was done with a force field taking into account accurately the entire solvation free energy (GBMV). Although the cluster number and content depends on the clustering RMSD cutoff value using the graph theory clustering, the best loop candidate remains the same for a wide range of cutoff values, implying that this value does not have any major impact on the result. Furthermore, in this range of cutoff values, the number of clusters exhibits a maximum, thus giving a maximum of choice to select a conformation.

MTSET Accessibility

A first consistent finding is that several residues of the second extracellular loop appear to be slightly more readily accessible in the E1 than in the E2 conformation. At first this seems to be surprising, since the E2 conformation is the state in which the “gate” controlling the cation access pathway from the outside is open. However, the 1SU4 (E1) and 1IWO (E2) structures of SERCA shows that in the E2 state, but not in E1, residues in this second loop are in close proximity to residues in the fourth extracellular loop linking M7 and M8 (Toyoshima and Nomura, 2002; Yudowski et al., 2003). This interaction that occurs between residues E314 and Y315 in L3/4 and V895 and N896 in L7/8 according to our model may somehow hinder the accessibility of several side chains in the E2 conformation. This lower accessibility in E2 must affect only rather large molecules, and not the monovalent cations for which the binding sites are accessible in the E2-P conformation. The gate responsible for cation occlusion is thus distinct from the extracellular part of the M3–M4 loop, which seems to modulate MTSET accessibility.

The Second Extracellular Loop Is a Major Determinant of the Affinity for Extracellular K⁺

Even if the extracellular part of the M3–M4 loop does not seem to constitute the occlusion gate, a second consistent finding was that mutations in this loop (E314C, Y315C, and I322C) or the binding of MTSET in the case of W317C, resulted in major modifications, an increase in most cases, of the apparent affinity for extracellular K⁺, the opposite of what we had observed for cysteine mutants (G803C and V805C) of the third extracellular loop in which a decrease in the apparent affinity for K⁺ was observed (Capendeguy and Horisberger, 2005). Eguchi et al. (2005) have studied the effects of mutation in the second extracellular loop and also observed alterations in the affinity for K⁺. For the W317E mutant, they reported only a minor modification of the K_{1/2}K⁺ of ATPase activity. However, the

other mutations in their study target different residues with different substitutions, and this makes it difficult to compare their results with ours, except for the fact that some of these mutations did affect the $K_{1/2}K^+$ of ATPase activity.

Changes in the apparent affinity for extracellular K^+ could be attributed in principle to changes in the binding sites themselves, to a global effect on the E1–E2 conformation equilibrium, or to a more specific alteration of the structure of the pathway leading from the extracellular solution to the binding site, and in particular the structure known as “the gate” that may control this access pathway.

From what we know of the general architecture of the α subunit, and the position of the second extracellular loop, any direct contribution of this domain to the potassium or sodium binding sites themselves seems very unlikely, since the binding sites are expected to be located much deeper within the protein (Ogawa and Toyoshima 2002). A global shift in the E1–E2 equilibrium, unrelated to the modification of the intrinsic cation affinity, also seems to be unlikely for the following reasons. First, results of the ouabain-sensitive transient current measurements indicate no significant change in the E1 to E2 equilibrium of the Na^+ -translocating limb of the cycle, or only a moderate shift toward the E1 conformation after MTSET treatment in the case of W317C and I322C, and whereas such a shift would be expected to induce a decrease in the apparent affinity for extracellular K^+ , the opposite is in fact observed. Second, an increase of the E2(K) to E1 rate would tend to increase V_{max} , whereas the opposite is in fact observed (increase in affinity is associated with a decrease in the maximum turnover). We therefore think that the effects of the mutations studied are not due, in general, to any major change in the E1–E2 conformation equilibrium, even though the possibility of some effect on this equilibrium cannot be excluded. How then can these mutations alter the potassium affinity and extracellular “gate” of the Na,K pump?

A simple explanation for the observed substantial changes involving just a single kinetic alteration would be that several mutations in the second extracellular loop lead to the stabilization of a closed state of the extracellular gate, once potassium ions have been bound to their sites. This would result in a stabilization of the potassium occlusion state E2(K). This stabilization would increase the apparent affinity for external K^+ , and could also reduce the overall turnover rate by slowing the K^+ deocclusion step, and thus decreasing the number of transport sites available for electrogenic Na^+ translocation. Obviously this hypothesis needs further experimental confirmation.

As illustrated in Fig. 7, during the E1 to E2 conformation change there is a rather large displacement of the whole M3–M4 hairpin: the position of the beginning of the M4 helix moves $>5 \text{ \AA}$ away from M6, and in the

same movement, the M3M4 loop is stretched due to increased separation between the anchor points (by 6.5 \AA). These movements are associated with a rotation of M4, which is clearly demonstrated by the change in the position of I322. All this reorganization of the M3 and M4 helices could result in the opening or closing of a gate located close to the narrowest part of the cation pathway, corresponding to the level of T804 (Artigas et al., 2005). Mutations or other alterations in the second extracellular loop are therefore expected to lead to structural constraints on this loop and thereby influence the state of the extracellular side of the gate.

Access of Na^+ and K^+ Ions

It is worth pointing out that neither the mutations nor the binding of MTSET to the studied positions had any major impact on the variables linked to Na^+ transport, in contrast to their marked effects on the apparent affinity for K^+ . Apart from the effect of MTSET on W317C, only small displacements of the $V_{1/2}$ of the presteady-state currents resulted (Fig. 6). The competitive effect of extracellular Na^+ on $K_{1/2}K^+$ was present in all mutants before and after MTSET treatment (compare Figs. 4 and 5), and the apparent affinity for K^+ was modified in a qualitatively similar manner in both the presence and the absence of extracellular Na^+ . These observations are in clear contrast to those for mutant E961A, and for other mutants at M9, M5, and M6 (Li et al., 2005), suggesting that the second extracellular loop has little influence on the voltage-dependent release/binding of extracellular Na^+ .

To conclude, we have shown that cysteine mutations or derivatization of the substituted cysteines in the second extracellular loop result in major changes in the apparent affinity for extracellular K^+ , and that the accessibility of several positions in this loop are dependent on the conformation state of Na,K-ATPase. After excluding other possible explanations, such as shift in global conformational equilibrium or alteration of the competitive binding of extracellular Na^+ , we propose that the second extracellular loop is functionally linked with the gate that controls the access of K^+ ions to their binding sites.

This work was funded by the Swiss National Fund grant 31-65441.01 to J.-D. Horisberger.

Olaf S. Andersen served as editor.

Submitted: 29 September 2005

Accepted: 7 February 2006

REFERENCES

- Apell, H.-J., and S.J.D. Karlish. 2001. Functional properties of Na,K-ATPase, and their structural implications, as detected with biophysical techniques. *J. Membr. Biol.* 180:1–9.
- Artigas, P., N. Reyes, and D.C. Gadsby. 2005. Na,K-ATPase ion translocation pathway. *J. Gen. Physiol.* 126:4A (Abstr.).
- Brooks, B.R., R.E. Brucoleri, B.D. Olafson, D.J. States, S. Swaminathan, and M. Karplus. 1983. Charmm-a program for

- macromolecular energy, minimization, and dynamics calculations. *J. Comput. Chem.* 4:187–217.
- Canessa, C.M., J.-D. Horisberger, and B.C. Rossier. 1993. Mutation of a tyrosine in the H3-H4 ectodomain of Na,K-ATPase confers ouabain resistance. *J. Biol. Chem.* 268:17722–17726.
- Capendeguy, O., and J.-D. Horisberger. 2005. The role of the third extracellular loop of the Na,K-ATPase α subunit in a luminal gating mechanism. *J. Physiol.* 565:207–218.
- Chamberlain, A.K., Y. Lee, S. Kim, and J.U. Bowie. 2004. Snorkeling preferences foster an amino acid composition bias in transmembrane helices. *J. Mol. Biol.* 339:471–479.
- Eguchi, H., K. Takeda, W. Schwarz, A. Shirahata, and M. Kawamura. 2005. Involvement in K^+ access of Leu(318) at the extracellular domain flanking M3 and M4 of the Na^+, K^+ -ATPase α -subunit. *Biochem. Biophys. Res. Commun.* 330:611–614.
- Fagerberg, T., J.C. Cerrotini, and O. Michielin. 2006. Structural prediction of peptides bound to MHC class I. *J. Mol. Biol.* In press.
- Forbush, B., III. 1987. Rapid release of ^{42}K or ^{86}Rb from two distinct transport sites on the Na, K-pump in the presence of Pi or vanadate. *J. Biol. Chem.* 262:11116–11127.
- Geering, K., I. Theulaz, F. Verrey, M.T. Häuptle, and B.C. Rossier. 1989. A role for the β -subunit in the expression of functional Na^+, K^+ -ATPase in *Xenopus* oocytes. *Am. J. Physiol.* 257:C851–C858.
- Granseth, E., G. Von Heijne, and A. Elofsson. 2005. A study of the membrane-water interface region of membrane proteins. *J. Mol. Biol.* 346:377–385.
- Guennoun, S., and J.-D. Horisberger. 2000. Structure of the 5th transmembrane segment of the Na,K-ATPase alpha subunit: a cysteine-scanning mutagenesis study. *FEBS Lett.* 482:144–148.
- Guennoun, S., and J.-D. Horisberger. 2002. Cysteine-scanning mutagenesis study of the sixth transmembrane segment of the Na,K-ATPase alpha subunit. *FEBS Lett.* 513:277–281.
- Horisberger, J.-D. 2004. Recent insights into the structure and mechanism of the sodium pump. *Physiology (Bethesda)*. 19:377–387.
- Horisberger, J.-D., and S. Kharoubi-Hess. 2002. Functional differences between α subunit isoforms of the rat Na,K-ATPase expressed in *Xenopus* oocytes. *J. Physiol.* 539:669–680.
- Horisberger, J.-D., S. Kharoubi-Hess, S. Guennoun, and O. Michielin. 2004. The 4th transmembrane segment of the Na,K-ATPase α subunit: a systematic mutagenesis study. *J. Biol. Chem.* 279:29542–29550.
- Jaisser, F., C.M. Canessa, J.-D. Horisberger, and B.C. Rossier. 1992. Primary sequence and functional expression of a novel ouabain-resistant Na,K-ATPase. *J. Biol. Chem.* 267:16895–16903.
- Jaisser, F., P. Jaunin, K. Geering, B.C. Rossier, and J.-D. Horisberger. 1994. Modulation of the Na,K-pump function by the β -subunit isoforms. *J. Gen. Physiol.* 103:605–623.
- Jaunin, P., J.-D. Horisberger, K. Richter, P.J. Good, B.C. Rossier, and K. Geering. 1992. Processing, intracellular transport and functional expression of endogenous and exogenous α - β Na,K-ATPase complexes in *Xenopus* oocytes. *J. Biol. Chem.* 267:577–585.
- Jorgensen, P.L., K.O. Hakansson, and S.J.D. Karlsh. 2003. Structure and mechanism of Na,K-ATPase: functional sites and their interactions. *Annu. Rev. Physiol.* 65:817–849.
- Killian, J.A., and G. Von Heijne. 2000. How proteins adapt to a membrane-water interface. *Trends Biochem. Sci.* 25:429–434.
- Laskowski, R.A., M.W. MacArthur, D.S. Moss, and J.M. Thornton. 1993. PROCHECK: a program to check the stereochemical quality of protein structures. *J. Appl. Cryst.* 26:283–291.
- Li, C., O. Capendeguy, K. Geering, and J.-D. Horisberger. 2005. A third Na^+ binding site in the sodium pump. *Proc. Natl. Acad. Sci. USA.* 102:12706–12711.
- Nakao, M., and D.C. Gadsby. 1986. Voltage dependence of the Na translocation by the Na/K pump. *Nature.* 323:628–630.
- Ogawa, H., and C. Toyoshima. 2002. Homology modeling of the cation binding sites of the Na^+, K^+ -ATPase. *Proc. Natl. Acad. Sci. USA.* 99:15977–15982.
- Qiu, L.Y., E. Krieger, G. Schaftenaar, H.G.P. Swarts, P.H.G.M. Willems, J.J.H.H. De Pont, and J.B. Koenderink. 2005. Reconstruction of the complete ouabain-binding pocket of Na,K-ATPase in gastric H,K-ATPase by substitution of only seven amino acids. *J. Biol. Chem.* 280:32349–32355.
- Rakowski, R.F. 1993. Charge movement by the Na/K pump in *Xenopus* oocytes. *J. Gen. Physiol.* 101:117–144.
- Rakowski, R.F., L.A. Vasilets, J. LaTona, and W. Schwarz. 1991. A negative slope in the current-voltage relationship of the Na^+/K^+ pump in *Xenopus* oocytes produced by reduction of external $[K^+]$. *J. Membr. Biol.* 121:177–187.
- Sorensen, T.L.M., J.V. Moller, and P. Nissen. 2004. Phosphoryl transfer and calcium ion occlusion in the calcium pump. *Science.* 304:1672–1675.
- Toyoshima, C., and G. Inesi. 2004. Structural basis of ion pumping by Ca^{2+} -ATPase of the sarcoplasmic reticulum. *Annu. Rev. Biochem.* 73:269–292.
- Toyoshima, C., M. Nakasako, H. Nomura, and H. Ogawa. 2000. Crystal structure of the calcium pump of sarcoplasmic reticulum at 2.6 Å resolution. *Nature.* 405:647–655.
- Toyoshima, C., and H. Nomura. 2002. Structural changes in the calcium pump accompanying the dissociation of calcium. *Nature.* 418:605–611.
- Ulmschneider, M.B., and M.S.P. Sansom. 2001. Amino acid distributions in integral membrane protein structures. *Biochim. Biophys. Acta.* 1512:1–14.
- Yudowski, G.A., M. Bar Shimon, D.M. Tal, R.M. Gonzalez-Lebrero, R.C. Rossi, P.J. Garrahan, L.A. Beauge, and S.J.D. Karlsh. 2003. Evidence for tryptophan residues in the cation transport path of the Na^+, K^+ -ATPase. *Biochemistry.* 42:10212–10222.